Real-time control and parameters estimation using the Novint Falcon parallel robot as experimental platform

Iván Torres-Rodríguez * **José Daniel Castro-Díaz** *
Marco A. Arteaga-Pérez **

* *Facultad de Ingeniería, UNAM, Ciudad de México, México. C.P. 04510 (email: ivantr18@hotmail.com)*
** *Departamento de Control y Robótica, Facultad de Ingeniería, UNAM, Ciudad de México, México C.P. 04510 (email: daniel_castro@comunidad.unam.mx, marteagp@unam.mx)*

Abstract: The Novint Falcon parallel robot is an inexpensive robot created originally for the videogaming industry. Its closed kinematic structure allows to recreate a wide range of forces which the serial structure robots counterparts cannot, making it suitable for haptic applications where the principal task is to reproduce a resultant force in its end effector with the aim to recreate tactil sensations from virtual objects. Nevertheless, the experimental use of this mechanism from the linear and non-linear control theory approach has been little exploited. This work explores the Novint Falcon robot capabilities as an easily accessible control research platform by implementing two control algorithms and comparing its performance.

Keywords: Parallel robot, PID control, adaptive control, performance comparison.

1. INTRODUCTION

Robot manipulators are systems in which many control algorithms have been designed. Due to their intrinsic characteristic as nonlineariry and parametric variation they are excellent experimental platforms to study, develop, prove and improve such algorithms. Beyond the industrial applications for which they was originally created, they have become an essential part of a numerous scientific laboratories around the world. However, the high cost of robot manipulators devices and its industrial closed architecture make difficult the research labor, driving scientist to look for another available options in the market.
The parallel robot Novint Falcon is a low inertia inexpensive 3 DOF robot created originally as a video game interface. Its principal task in this area is to transmit forces in order to increase the user immersion degree and enhance his or her interactive experience, which is performed through the robot closed-kinematic structure and preprogrammed force feedback algorithms. Nevertheless, its easy set up and versatility has extended its use to cutting edge scientific purposes. For example, in Zhaohong et al. (2010) it is used as a motor rehabilitation trainer for stroke patients with handwriting difficulties so that they can improve their motor skill, postural stability and hand-eye coordination. In Ondrej and Manic (2011) a fuzzy force-feedback augmentation for manual control of multi-robot systems is designed using the Novint Falcon robot as master device in a teleoperated system. Moreover, in the review stated by Coles et al. (2011) is reported two Novint Falcon robots that are specifically configured to give 5 DOF to a single drill handle which is used in virtual reality surgical simulators while the platform haptic capabilities are tested in Rodríguez and Velázquez (2012) by using the device to render forces from simple virtual shapes that users can explore actively, and in Torres-Rodríguez et al. (2017) by creating a virtual reality application with force rendering using a spring-damper equation as penalty method. These works exemplify that haptics is the major field where a large number of applications are developed using the parallel Novint Falcon robot, while a reduced number in the literature address the control theory approach that had been largely studied in industrial-type serial manipulators. Just to mention a few, Stamper (1997) provides a mathematical analysis which results in equations for the robot forward and inverse kinematics. On the other hand, Martin and Hiller (2009) present a delineation of the Novint Falcon for manipulation applications, including a motors characterization which is not provided by the manufacturer. Furthermore Karbasizadeh et al. (2016) present a dynamic identification using a CAD model and assigning properties of its constituent parts and by using a white box identification procedure, the unknown parameters in closed-form dynamic model of the robot are identified in a simulation environment.
As far as the authors knowledge, the most control-oriented paper is Block et al. (2013) which describes the development of an embedded system to control the Novint mechanism as a robotic actuator and subsequently using it to control three independent Novint Falcons for a ball-on-plate experiment. However this work focuses mostly on describing the system hardware instrumentation and

only a PID linear control is tested.
In the aforementioned works the principal aim is to mathematically describe the parallel structure of the Novint Falcon robot and its properties. Additionally, some parameters are obtained by dynamic characterization, including those of the motors and the dynamic model by means of digital simulations. Nevertheless, no non-linear control algorithms are implemented experimentally. In contrast, in this work we present the designs of a linear PID control and an non-linear adaptive control with the aim to verify the suitability of the Novin Falcon as an experimental platform for control theory purposes. Moreover, we make a performance comparison of both controllers, setting down the principal differences between them.
The paper is organized as follows. In Section 2, a mathematical model for the Novint Falcon parallel robot is introduced as well as some of its properties. Section 3 presents the design of two control algorithms from the linear an non-linear control theory approach. The experimental validation and results are included in Section 4 and finally, some concluding remarks are given in Section 5.

2. DYNAMIC MODEL AND PROPERTIES

The dynamic model of the paralel robot can be described as

$$\boldsymbol{H}(\boldsymbol{q})\ddot{\boldsymbol{q}} + \boldsymbol{C}(\boldsymbol{q},\dot{\boldsymbol{q}})\dot{\boldsymbol{q}} + \boldsymbol{D}\dot{\boldsymbol{q}} + \boldsymbol{g}(\boldsymbol{q}) = \boldsymbol{\tau} \quad (1)$$

where $\boldsymbol{q} \in \Re^n$ is the vector of generalized joint coordinates, $\boldsymbol{H}(\boldsymbol{q}) \in \Re^{n\times n}$ is the positive definite inertia matrix, $\boldsymbol{C}(\boldsymbol{q},\dot{\boldsymbol{q}})\dot{\boldsymbol{q}} \in \Re^n$ represents the Coriolis and centrifugal torques, $\boldsymbol{D}\dot{\boldsymbol{q}} \in \Re^n$ is the vector of viscous friction with $\boldsymbol{D} \in \Re^{n\times n}$ being a positive definite matrix with viscous friction coefficents, $\boldsymbol{g}(\boldsymbol{q}) \in \Re^n$ is the the vector of gravitational forces and $\boldsymbol{\tau} \in \Re^n$ is the control input vector.

Equation (1) describe the motion of the system and it have the following properties:

Property 1. The inertia matrix $\boldsymbol{H}_i(\boldsymbol{q}_i)$ satisfies

$$\lambda_{\mathrm{h}i}\|\boldsymbol{x}_i\|^2 \le \boldsymbol{x}_i^{\mathrm{T}}\boldsymbol{H}_i(\boldsymbol{q}_i)\boldsymbol{x}_i \le \lambda_{\mathrm{H}i}\|\boldsymbol{x}_i\|^2, \quad \forall \boldsymbol{x}_i, \in \Re^n$$

where

$$\lambda_{\mathrm{h}i} = \min_{\forall \boldsymbol{q}_i} \lambda_{\min}\{\boldsymbol{H}_i(\boldsymbol{q}_i)\}$$
$$\lambda_{\mathrm{H}i} = \max_{\forall \boldsymbol{q}_i} \lambda_{\max}\{\boldsymbol{H}_i(\boldsymbol{q}_i)\}$$

for $i = 1, \ldots, n$. △

Property 2. The matrix $\dot{\boldsymbol{H}}_i(\boldsymbol{q}_i) - 2\boldsymbol{C}_i(\boldsymbol{q}_i,\dot{\boldsymbol{q}}_i)$ is skew-symmetric. △

In a parallel robot not all joints can be controlled independently due to its close chain structure. The Novint Falcon have three actuated joints in its base that are labeled as θ_{11}, θ_{12} and θ_{13}, representing the joint vector $\boldsymbol{q}$.
The mapping between the velocity end efector $\dot{\boldsymbol{x}}$ and the joint velocity $\dot{\boldsymbol{q}}$ is

$$\dot{\boldsymbol{q}} = \boldsymbol{J}(\boldsymbol{q})\dot{\boldsymbol{x}} \quad (2)$$

where $\boldsymbol{J}(\boldsymbol{q}) \in \Re^{n\times m}$ is the robot Jacobian matrix. It is evident that in a parallel robot the Jacobian matrix is inverse to a serial robot one.

The dynamic model stated by the equation (1) can be represented as the product between a matrix $\boldsymbol{Y}$ known as regressor and the parameters vector $\boldsymbol{\theta}$ in the form (Slotine and Li, 1987)

$$\boldsymbol{H}(\boldsymbol{q})\ddot{\boldsymbol{q}} + \boldsymbol{C}(\boldsymbol{q},\dot{\boldsymbol{q}})\dot{\boldsymbol{q}} + \boldsymbol{D}\dot{\boldsymbol{q}} + \boldsymbol{g}(\boldsymbol{q}) = \boldsymbol{Y}(\boldsymbol{q},\dot{\boldsymbol{q}},\ddot{\boldsymbol{q}})\boldsymbol{\theta} \quad (3)$$

where $\boldsymbol{Y}(\boldsymbol{q},\dot{\boldsymbol{q}},\ddot{\boldsymbol{q}})$ is known and depends on the measurables system signals and can be expressed as

$$\boldsymbol{Y} = [\boldsymbol{Y}_{\mathrm{H}} + \boldsymbol{Y}_{\mathrm{C}} \quad \boldsymbol{Y}_{\mathrm{D}} \quad \boldsymbol{Y}_{\mathrm{g}}]$$

where

$$\boldsymbol{Y}_{\mathrm{H}} = \left[\ddot{\boldsymbol{q}} \quad (\boldsymbol{J}^{\mathrm{T}})^{-1}\boldsymbol{J}^{-1}\ddot{\boldsymbol{q}}\right],$$
$$\boldsymbol{Y}_{\mathrm{C}} = \left[\boldsymbol{0} \quad (\boldsymbol{J}^{\mathrm{T}})^{-1}\frac{d}{dt}(\boldsymbol{J}^{-1})\dot{\boldsymbol{q}}\right],$$
$$\boldsymbol{Y}_{\mathrm{D}} = \dot{\boldsymbol{q}} \quad \text{and}$$
$$\boldsymbol{Y}_{\mathrm{g}} = \begin{bmatrix} -\sin(\phi_1)\sin(\theta_{11}) & 0 \\ -\sin(\phi_2)\sin(\theta_{12}) & (\boldsymbol{J}^{\mathrm{T}})^{-1} \\ -\sin(\phi_3)\sin(\theta_{13}) & 0 \end{bmatrix}.$$

and where ϕ_i for $i = 1, 2, 3$ are kinematic parameters. The sum of the matrix $\boldsymbol{Y}_{\mathrm{H}}$ and $\boldsymbol{Y}_{\mathrm{C}}$ is due to the inertia matrix and Coriolis matrix share some parameters.
Finally, the vector of parameters has the form

$$\boldsymbol{\theta} = \begin{bmatrix} I_A \\ m \\ b_A \\ ag(\frac{1}{2}m_a + m_b) \\ mg \end{bmatrix}, \quad (4)$$

where $\boldsymbol{H}(\boldsymbol{q})$, $\boldsymbol{C}(\boldsymbol{q},\dot{\boldsymbol{q}})\dot{\boldsymbol{q}}$, $\boldsymbol{D}$ and $\boldsymbol{g}(\boldsymbol{q})$ are lineally dependent of $\boldsymbol{\theta}$. The physical meaning of this vector can be found in Torres-Rodríguez (2017) as well as the Novint Falcon kinematic and dynamic properties.

3. CONTROLLERS DESIGN

The objective of this section is to design a PID control and an adaptive control in order to make a performance comparison between them and show that the Novint Falcon parallel robot is suitable as experimental platform for non-linear control algorithms.

3.1 PID control

Considering the tracking error of the system (1) as

$$\tilde{\boldsymbol{q}} = \boldsymbol{q} - \boldsymbol{q}_{\mathrm{d}} \quad (5)$$

where $\boldsymbol{q}_{\mathrm{d}}$ is the desired joint position with first and second bounded derivatives, the well known PID control equation is

$$\boldsymbol{\tau} = \boldsymbol{K}_P\tilde{\boldsymbol{q}} + \boldsymbol{K}_I\int_0^t \tilde{\boldsymbol{q}}\ dt + \boldsymbol{K}_D\frac{d\tilde{\boldsymbol{q}}}{dt}$$

where $\boldsymbol{\tau}$ is the torque input to be applied to the Novint Falcon joints and $\boldsymbol{K}_P$, $\boldsymbol{K}_I$ and $\boldsymbol{K}_D$ are diagonal positive gain matrices.

3.2 Adaptive Control

A position tracking adaptive control was designed. Considering the model of the equation (3) and the tracking error (5) the parametric error is defined as

$$\tilde{\boldsymbol{\theta}} = \hat{\boldsymbol{\theta}} - \boldsymbol{\theta} \quad (6)$$

where $\hat{(\cdot)}$ is the estimated of $(\cdot)$. On the other hand it is necessary consider a velocity tracking reference as

$$\dot{\boldsymbol{q}}_{\mathrm{r}} = \dot{\boldsymbol{q}}_{\mathrm{d}} - \boldsymbol{\Lambda}\tilde{\boldsymbol{q}} \tag{7}$$

where $\boldsymbol{\Lambda}$ is a skew symetric positive definite matrix and

$$\boldsymbol{s} = \dot{\boldsymbol{q}} - \dot{\boldsymbol{q}}_{\mathrm{r}} \tag{8}$$

a variable velocity error.
Since the stability of the system depends on both the control and adaptation laws, a Lyapunov candidate function is proposed

$$\boldsymbol{V}(t) = \frac{1}{2}(\boldsymbol{s}^{\mathrm{T}}\boldsymbol{H}\boldsymbol{s} + \tilde{\boldsymbol{\theta}}^{\mathrm{T}}\boldsymbol{\Gamma}^{-1}\tilde{\boldsymbol{\theta}}). \tag{9}$$

The derivative of this equation is

$$\dot{\boldsymbol{V}}(t) = \boldsymbol{s}^{\mathrm{T}}(\boldsymbol{H}\ddot{\boldsymbol{q}} - \boldsymbol{H}\ddot{\boldsymbol{q}}_{\mathrm{r}}) + \frac{1}{2}\boldsymbol{s}^{\mathrm{T}}\dot{\boldsymbol{H}}\boldsymbol{s} + \dot{\tilde{\boldsymbol{\theta}}}^{\mathrm{T}}\boldsymbol{\Gamma}^{-1}\tilde{\boldsymbol{\theta}}. \tag{10}$$

From equation (1) we have

$$\boldsymbol{H}\ddot{\boldsymbol{q}} = \boldsymbol{\tau} - \boldsymbol{C}\dot{\boldsymbol{q}} - \boldsymbol{D}\dot{\boldsymbol{q}} - \boldsymbol{g} \tag{11}$$

By substituting (11) in (10) and due to Property 2, the term $\frac{1}{2}\boldsymbol{s}^{T}\dot{\boldsymbol{H}}\boldsymbol{s}$ is eliminated resulting in

$$\dot{\boldsymbol{V}}(t) = \boldsymbol{s}^{\mathrm{T}}(\boldsymbol{\tau} - \boldsymbol{H}\ddot{\boldsymbol{q}}_{\mathrm{r}} - \boldsymbol{C}\dot{\boldsymbol{q}}_{\mathrm{r}} - \boldsymbol{D}\dot{\boldsymbol{q}}_{\mathrm{r}} - \boldsymbol{g} - \boldsymbol{D}\boldsymbol{s}) + \dot{\tilde{\boldsymbol{\theta}}}^{\mathrm{T}}\boldsymbol{\Gamma}^{-1}\tilde{\boldsymbol{\theta}}. \tag{12}$$

Given the above equations, the proposed adaptive control algorithm is given by

$$\boldsymbol{\tau} = \boldsymbol{Y}\hat{\boldsymbol{\theta}} - \boldsymbol{K}\boldsymbol{s}$$

where the first term eliminates the system dynamics by means of the regressor and the second one is a PD feedback term. Finally, the adaptive law

$$\dot{\hat{\boldsymbol{\theta}}} = -\boldsymbol{\Gamma}\boldsymbol{Y}^{\mathrm{T}}\boldsymbol{s}.$$

is proposed.
By substituting (6) in (12) we have

$$\dot{\boldsymbol{V}}(t) = \boldsymbol{s}^{\mathrm{T}}\boldsymbol{Y}\hat{\boldsymbol{\theta}} - \boldsymbol{s}^{\mathrm{T}}(\boldsymbol{K} + \boldsymbol{D})\boldsymbol{s} + \dot{\tilde{\boldsymbol{\theta}}}^{\mathrm{T}}\boldsymbol{\Gamma}^{-1}\tilde{\boldsymbol{\theta}},$$

and finally

$$\dot{\boldsymbol{V}}(t) = -\boldsymbol{s}^{\mathrm{T}}(\boldsymbol{K} + \boldsymbol{D})\boldsymbol{s}$$

which is a quadratic positive semidefinite equation.

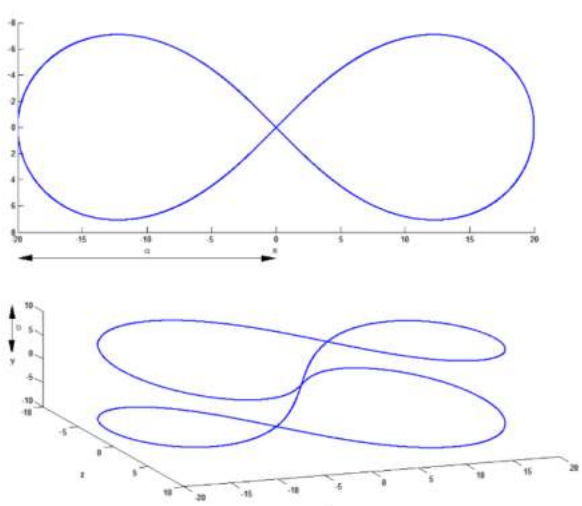

Fig. 1. Bernoulli Lemniscate

3.3 *Desired Trajectory*

The trajectory is divided in two segments. The first one is given by a polinomial equation of the form

$$q(t) = a_0 + a_1 t + a_2 t^2 + a_3 t^3 + a_4 t^4 + a_5 t^5.$$

The second one is a Bernoulli Lemniscate as shown in Figure 1 and given by the parametric equations

$$x = \frac{a\cos(\omega t)}{1 + \sin^2(\omega t)}$$

$$y = b\cos(0.5\omega t)$$

$$z = \frac{a\sin(\omega t)\cos(\omega t)}{1 + \sin^2(\omega t)}$$

where ω is the angular velocity, a is the half of the total lemniscate width and b is the depth over the y axis.

4. EXPERIMENTAL RESULTS

To verify the performance of the control algorithms presented in Section 3, a set of experiments were carried out. The test-bed shown in Figure 3 is composed for the Novint Falcon robot and a PC with Windows 7 using the library Haptik 7 as communication interface with the application programmed in C++. The physic connection was made through USB 2.0 protocol, however, it is important to highlight that a Visual Studio 2015 multimedia timer was used so that real-time experimentation was achieved at a 5 [ms] sample period.

4.1 *PID controller*

The PID control scheme for experimental evaluation is shown in Figure 2. It was necessary to use the Jacobian matrix in the equation (2) at the controller output because the Haptik 7 library can send only forces to the robot Novint Falcon device. Thus, it is necessary to make a mapping between torques and forces by means of such matrix.
In order to correctly tune the PID gains, the equation

$$u(t) = k_p\left(e(t) + \frac{1}{T_i}\int_0^t e(t)dt + T_d\frac{de(t)}{dt}\right)$$

was used. This tuning was done through the Ziegler-Nichols method. In this case a critic gain was established in order to obtain a sustained oscillation as the system response in closed loop. By varying the critic gain and finding a critic oscillation period, the gains in Table 1 were obtained.

Gain	q_1	q_2	q_3
k_p	3.276	4.602	4.290
T_i [ms]	160	163	175
T_d [ms]	28.1	28.7	31

Table 1. PID control gains

The desired trajectory $\boldsymbol{q}_{\mathrm{d}}$ and the joint trajectory $\boldsymbol{q}$ are shown in Figure 4. As it can be appreciated a good position tracking is achieved in a 30 [s] experiment duration.

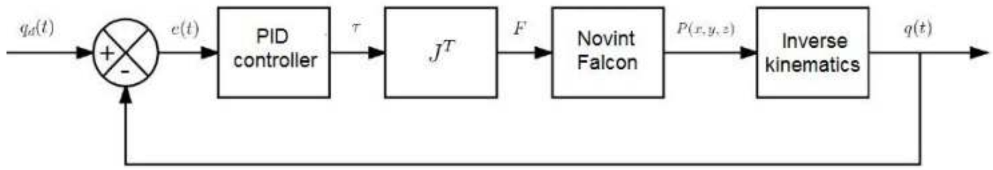

Fig. 2. PID control scheme

Fig. 3. Experimental test-bed

The first trajectory segment occurs from 0 to 4 [s] and the Bernoulli lemniscate occurs till the end with an oscillatory behavior. The control performance is shown in Figure 5

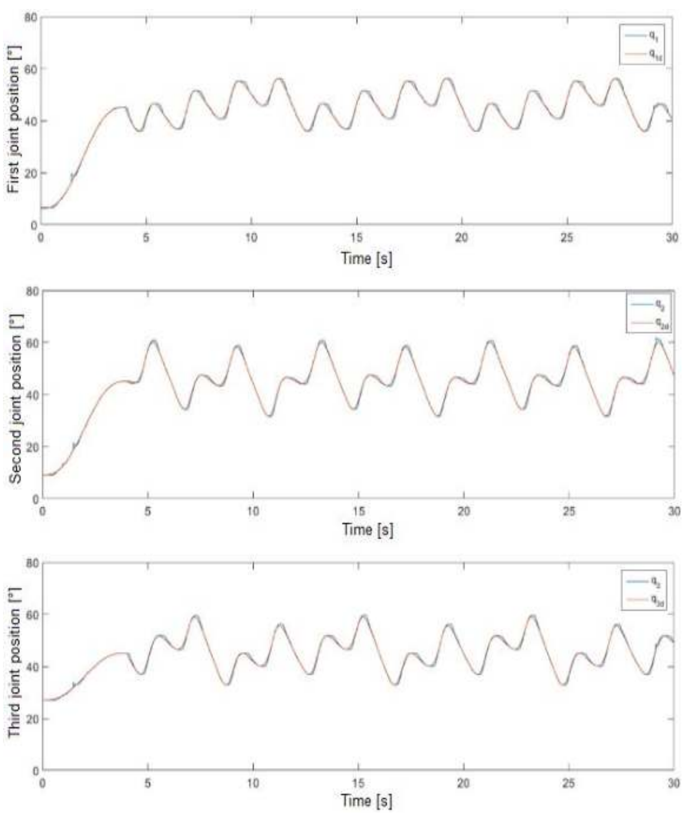

Fig. 4. PID control tracking

where the maximum error value is approximately 3.25 [°] and exist some impulses due to noise measurements and the use of numerical approximation to calculate the PID derivative.

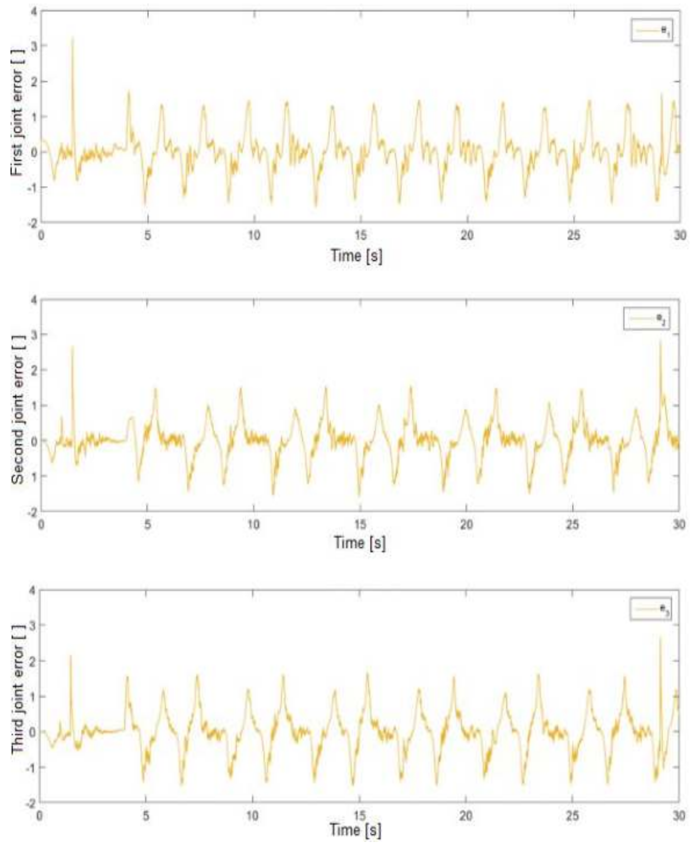

Fig. 5. PID control error tracking

4.2 Adaptive controller

The adaptive control scheme for experimental evaluation is shown in Figure 6 where the gains were tuned experimentally. The desired trajectory $\boldsymbol{q}_\mathrm{d}$ and the joint trajectory $\boldsymbol{q}$ are shown in Figure 7. As it can be appreciated a good position tracking is also achieved in a 30 [s] experiment duration. The first trajectory segment occurs from 0 to 4 [s] and the Bernoulli lemniscate occurs till the end. The control performance is shown in Figure 8 where the maximum error value is approximately 3 [°] and the error tends to zero as time advances. In this case there is not any impulses even when noise measurements also occur because of the use of a Levant differentiator which is robust to noise and theoretically exact. The vector parameters estimation of the equation (4) is shown

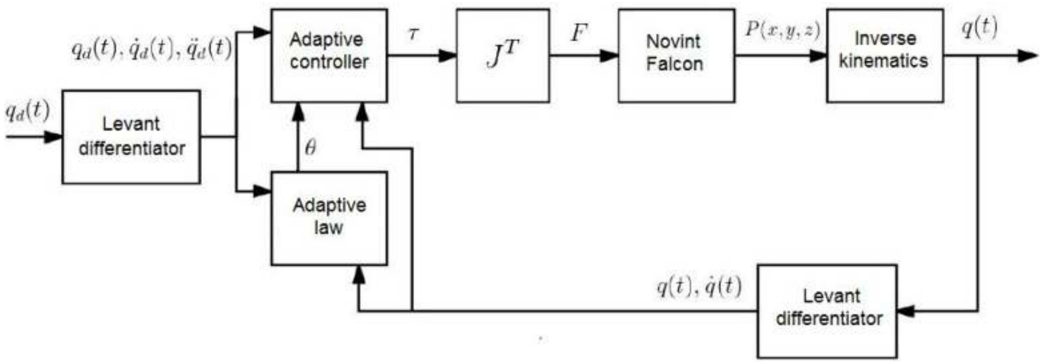

Fig. 6. Adaptive control scheme

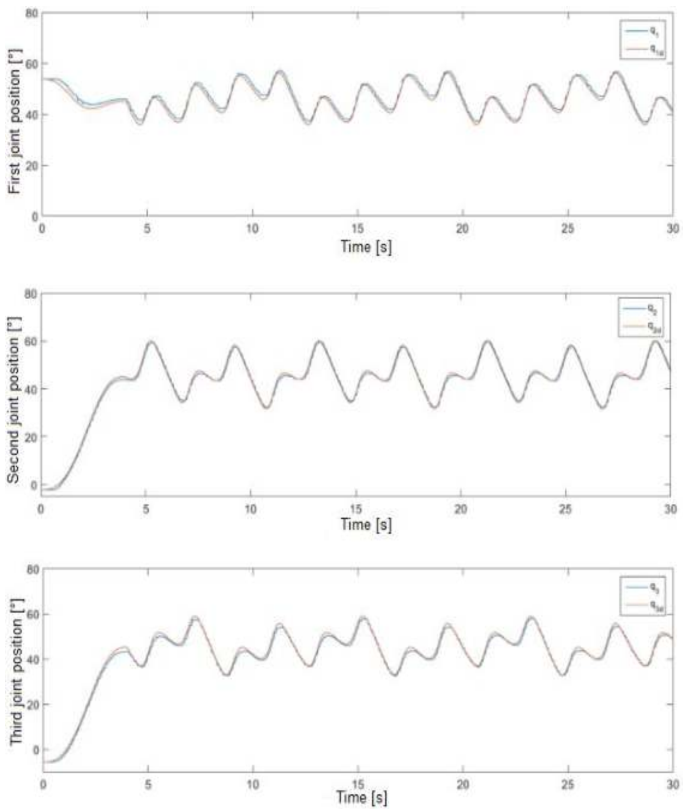

Fig. 7. Adaptive control performance

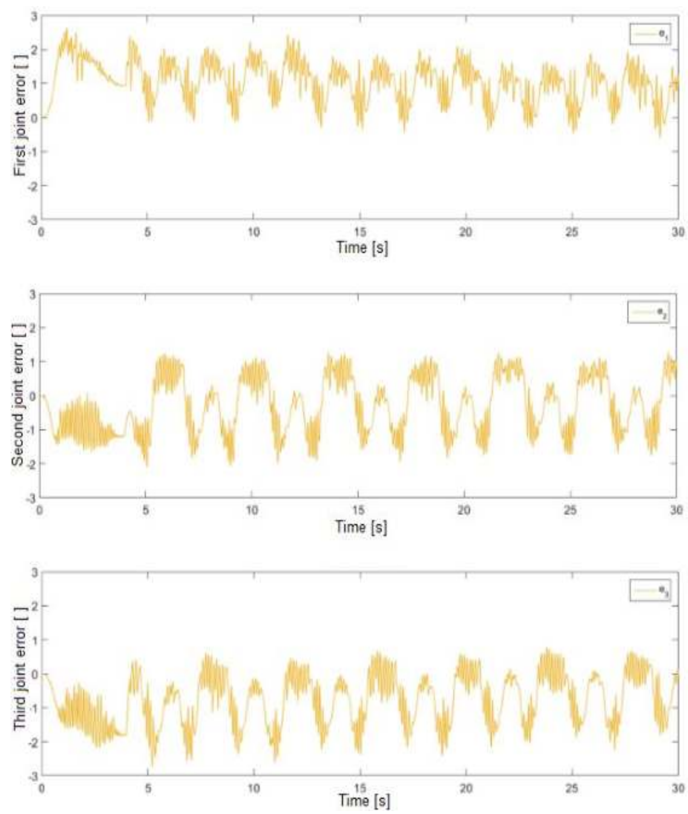

Fig. 8. Adaptive error tracking

in Figure 9. The parameter θ_1 is negative because the excitation signal of the system (in this case the desired trajectory) is not sufficiently rich in frequencies as Slotine and Li (1987) propose.

4.3 Results comparison

With the aim to carrying out an analytical comparison the root mean square error (RMSE) was used. The equation of this indicator is

$$\mathrm{RMSE} = \sqrt{\frac{1}{n}\sum_{i=1}^{n}(q - q_d)^2} \tag{13}$$

where n is the number of samples. The RMSE of every joint is shown in Table 2 for the PID and the adaptive controller as well as the maximum absolute error.

Controller	RMSE[°]			$\lvert e_{\max}\rvert$[°]		
	q_1	q_2	q_3	q_1	q_2	q_3
PID	0.56	0.52	0.57	3.25	2.82	2.66
Adaptive	1.2	0.69	0.9	2.62	1.69	2.34

Table 2. RMSE for a 30 [s] experiment

As it can be appreciated the RMSE of the PID controller is smaller than that of the adaptive controller, indicating, at a first sight, that PID performance is better. However, as we can see in Table 3 the adaptive controller get a better performance reaching 70 [s], showing 8 % and 4 %

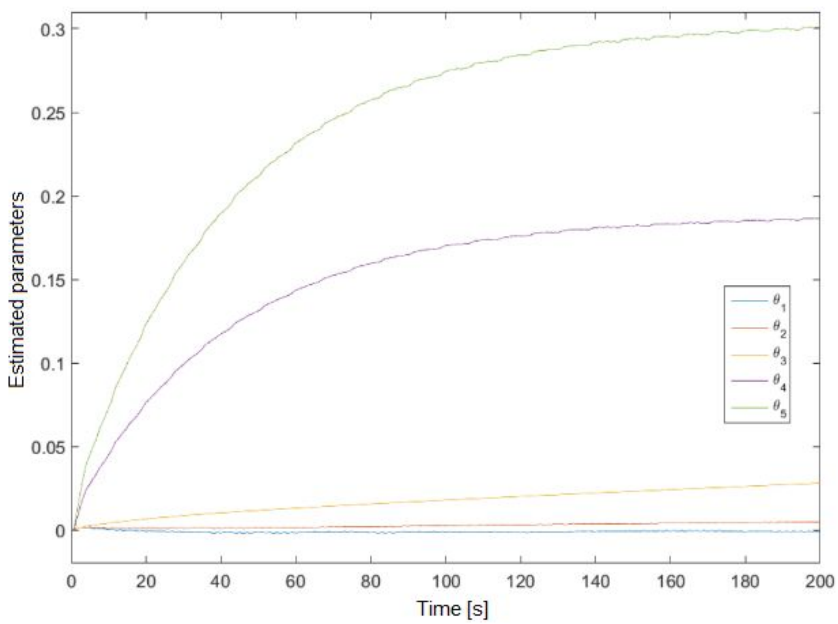

Fig. 9. Parameters estimation to 200 [s]

less RMSE respect to PID controller for joints 1 and 3 respectively while for joint 2 is 6.5 % more.

Controller	RMSE[°]			$\|e_{\max}\|$[°]		
	q_1	q_2	q_3	q_1	q_2	q_3
PID	0.56	0.52	0.57	3.25	2.82	2.66
Adaptive	0.51	0.56	0.55	1.41	1.23	1.4

Table 3. RMSE for a 70 [s] experiment.

With regard to the maximum absolute error, the adaptive controller has an error 56 %, 55 % and 47 % less in every joint with respect to PID controller. In this sense we can conclude that the former has a better performance than the latter but only when the experiment reaches at 70 [s] due to the time it takes to the adaptive law to estimate the vector of parameters.

5. CONCLUSIONS

In this paper we showed that parallel robot Novint Falcon is suitable as a control theory experimental platform. Even when this device was originally created for the videogaming industry, which explains its low price, it has been largely used in scentific laboratories where the principal study subject is the force rendering towards the user. In fact, this robot appear as haptic experimental platform in a wide range of works as an alternative to the high-costed industrial devices. Nevertheless the potential as a control theory platform as been little exploited. We proposed two control schemes, a classical PID control and an adaptive control, with which we demonstrate that the robot capabilities in this area are in the industrial manipulators level, where control theory experimentation has been developed vastly. As future work we propose to upgrade the Novint Falcon parallel structre by adding an spherical-wrist-type mechanism in order to allow not only position but orientation control also, and testing the modified robot experimental capabilities in control theory and haptic applications as well as the design and control of a teleoperated system using non-similar kinematic structure robots.

ACKNOWLEDGMENT

This work has been supported by the **DGAPA-UNAM** under grant **IN114617**.

REFERENCES

Block, D.J., Michelotti, M.B., and Sreenivas, R.S. (2013). Application of the Novint Falcon haptic device as an actuator in real-time control. *PALADYN Journal of Behavioral Robotics*, 182–193.

Coles, T., Meglan, D., and John, N. (2011). The Role of Haptics in Medical Training Simulators: A Survey of the State of the Art. *IEEE Transactions on Haptics*, 4(1), 51–66.

Karbasizadeh, N., Aflakiyan, A., Zarei, M., and Kalhor, A. (2016). Dynamic Identification of the Novint Falcon Haptic Device. *Proceedings of the 4th International Conference on Robotics and Mechatronics*, 518–523.

Martin, S. and Hiller, N. (2009). Characterisation of the Novint Falcon Haptic Device for Application as a Robot Manipulator. *Australian Conference on Robotics and Automation*.

Ondrej, L. and Manic, M. (2011). Fuzzy Force-Feedback Augmentation for Manual Control of Multirobot Systems. *IEEE Transactions on Industrial Electronics*, 58, 3213–3220.

Rodríguez, L. and Velázquez, R. (2012). Haptic Rendering of Virtual Shapes with the Novint Falcon. *Proceedings of the 2012 Iberoamerican Conference on Electronics and Computer Science*, 132–138.

Slotine, J.J.E. and Li, W. (1987). On the Adpative Control of Robot Manipulators. *International Journal of Robotics Reseach*, 6(3), 49–59.

Stamper, R. (1997). *A three degree of freedom parallel manipulator with only translational degrees of freedom.* Ph.D. thesis, University of Maryland.

Torres-Rodríguez, I. (2017). *Start up of the parallel robot Novint Falcon.* Master's thesis, Faculty of Engineering, UNAM.

Torres-Rodríguez, I., Castro-Díaz, J.D., and Pliego-Jiménez, J. (2017). The Novint Falcon parallel robot as experimental haptic platform. *Proceedings of the 2017 National Conference on Automatic Control*, 587–593.

Zhaohong, X., Hongliu, Y., and Shiju, Y. (2010). Motor rehabilitation training after stroke using haptic handwriting and games. *Proccedings of the 4th International Convention on Rehabilitation Engineering and Assistive Technology.*

